Journal of Alloys and Compounds 509 (2011) 827–830

Contents lists available at ScienceDirect

Journal of Alloys and Compounds

journal homepage: www.elsevier.com/locate/jallcom

Effects of Bi^{3+} doping on the optical properties of Er^{3+}:Y_2O_3

Mingzhu Yang[a], Yu Sui[a,b,*], Shipeng Wang[a], Xianjie Wang[a], Yang Wang[a], Shuchen Lü[c], Zhiguo Zhang[a], Zhiguo Liu[a], Tianquan Lü[a], Wanfa Liu[d]

[a] Center for Condensed Matter Science and Technology (CCMST), Department of Physics, Harbin Institute of Technology, Harbin 150001, People's Republic of China
[b] International Center for Materials Physics, Academia Sinica, Shenyang 110015, People's Republic of China
[c] Department of Physics, Harbin Normal University, Harbin 150001, People's Republic of China
[d] Dalian Institute of Chemical Physics, Dalian 116023, People's Republic of China

ARTICLE INFO

Article history:
Received 22 June 2010
Received in revised form 9 September 2010
Accepted 18 September 2010
Available online 25 September 2010

Keywords:
Luminescence
Optical materials
Optical properties
Sol–gel process

ABSTRACT

The influences of Bi^{3+} doping on the optical properties of Er^{3+}:Y_2O_3 are investigated under UV and IR excitations. The emission intensity of Er^{3+} is remarkably enhanced by the introduction of Bi^{3+} under both two excitations. The emission enhancement under UV excitation originates from the energy transfer from Bi^{3+} to Er^{3+}, while under IR excitation it can be attributed to the modification of the local crystal field around the Er^{3+}.

1. Introduction

Over the past several decades, considerable works have been carried out on the rare earth ions doped luminescent materials regarding their applications in illumination, color displays, and biomedical imaging [1–3]. Among luminescent rare earth ions, Er^{3+} is one of the most popular efficient ions, because its excited states ($^4I_{11/2}$) with long lifetimes can be easily populated by 980 nm irradiation [4,5]. As for the host for luminescent materials, most attention has been paid to oxide ceramics and nanopowders recently [6–8]. Y_2O_3 is a promising oxide host material due to its high melting point, high chemical stability and low phonon energy. Er^{3+}:Y_2O_3 has been established as one of the model systems for generating efficient upconversion radiation under 980 nm laser excitation [4,5].

As the emission of most luminescent materials does not have enough intensity, it is still a formidable challenge about how to improve the emission efficiency of these materials. It is known that doping of sensitizer ions or breaking of the crystal field symmetry can lead to the increase in the emission intensity of rare earth ions [9–11]. Bi^{3+} possesses a broad absorption band centering around 330 nm, and a broad emission band raging from 300 to 700 nm [12–14]. The emission band of Bi^{3+} overlaps with the $^4I_{15/2} \rightarrow {}^4F_{7/2}$ and $^4I_{15/2} \rightarrow {}^2H_{11/2}$ transitions of Er^{3+}, so Bi^{3+} can also be used as a sensitizer of Er^{3+} for the radiative energy transfer process. The broad absorb band of Bi^{3+} is beneficial to absorb more energy and enhance Er^{3+} emission under UV excitation. Moreover, as the radius of Bi^{3+} is larger than that of Y^{3+}, substitution of Y^{3+} with Bi^{3+} can modify the symmetry of crystal field in Y_2O_3, which is in favor of the enhancement of emission intensity.

In this study, Bi^{3+} is selected as codopant to enhance the luminescent efficiency of Er^{3+}. The emission intensity of Er^{3+} is increased under both 330 nm and 980 nm excitations. The relevant mechanisms are discussed in detail.

2. Experimental

Y_2O_3 powders doped with different concentrations of Er^{3+} and Bi^{3+} were prepared by a sol–gel combustion method. High purity Y_2O_3, Er_2O_3, Bi_2O_3 and $C_6H_8O_7{\cdot}H_2O$ were used as starting materials. First, stoichiometric Y_2O_3, Er_2O_3 and Bi_2O_3 were dissolved in HNO_3. Then $C_6H_8O_7{\cdot}H_2O$ was added to the mixed solution with the molar ratio of nitrate to citric acid to be 4:1. The resulting solution was heated at 80 °C in order to obtain a gel. Subsequently, the gel was rapidly heated to 200 °C and an autocombustion process took place. Finally, the precursor was calcined at 800 °C in air to obtain Er^{3+} and Bi^{3+} codoped Y_2O_3 powders. The XRD patterns of the powders were recorded by a Rigaku D/max-γB diffractrometer using Cu Kα radiation (λ = 0.15418 nm). The content of Bi^{3+} was determined by EDS measurement, and the results show that the Bi^{3+} is nearly in stoichiometric. The Stokes emission measurements were performed on Hitachi F-4500 Fluorescence Spectrophotometer at room temperature. The upconversion emission spectra were measured by a power controllable 980 diode laser and detected with a lens-coupled monochromator with an attached photomultiplier.

* Corresponding author at: Center for Condensed Matter Science and Technology (CCMST), Department of Physics, Harbin Institute of Technology, Harbin 150001, People's Republic of China. Tel.: +86 45186418403.
E-mail address: suiyu@hit.edu.cn (Y. Sui).

0925-8388/$ – see front matter © 2010 Elsevier B.V. All rights reserved.
doi:10.1016/j.jallcom.2010.09.100

Table 1
The lattice parameter of Y_2O_3 doped with different contents of Er^{3+} and Bi^{3+}: (a) Bi^{3+}:Y_2O_3; (b) Er^{3+}:Y_2O_3; (c) 1.0 mol% Bi^{3+} codoped Er^{3+}:Y_2O_3; (d) 1.5 mol% Bi^{3+} codoped Er^{3+}:Y_2O_3; (e) 2.0 mol% Bi^{3+} codoped Er^{3+}:Y_2O_3; (f) 2.5 mol% Bi^{3+} codoped Er^{3+}:Y_2O_3; (g) 3.0 mol% Bi^{3+} codoped Er^{3+}:Y_2O_3.

Samples	a	b	c	d	e	f	g
Lattice parameter (Å)	10.606	10.603	10.605	10.608	10.610	10.615	10.618

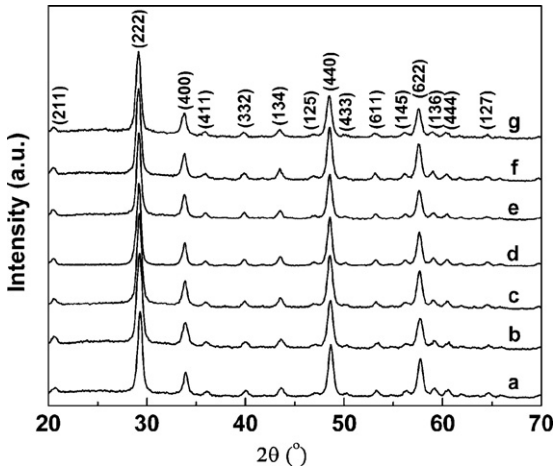

Fig. 1. XRD patterns of Y_2O_3 powders doped with different concentrations of Er^{3+} and Bi^{3+}: (a) Bi^{3+}:Y_2O_3; (b) Er^{3+}:Y_2O_3; (c) 1.0 mol% Bi^{3+} codoped Er^{3+}:Y_2O_3; (d) 1.5 mol% Bi^{3+} codoped Er^{3+}:Y_2O_3; (e) 2.0 mol% Bi^{3+} codoped Er^{3+}:Y_2O_3; (f) 2.5 mol% Bi^{3+} codoped Er^{3+}:Y_2O_3; (g) 3.0 mol% Bi^{3+} codoped Er^{3+}:Y_2O_3.

3. Results and discussion

The XRD patterns of Y_2O_3 doped with different concentrations of Er^{3+} and Bi^{3+} are shown in Fig. 1. The XRD data confirm that all samples are single phase with cubic structure (JPDS No. 86-1107). The lattice parameters are listed in Table 1. The results show that Bi^{3+} and Er^{3+} were successfully doped into Y_2O_3 host, and with the increase in Bi^{3+} content, the lattice parameter increases since the ion radius of Bi^{3+} is larger than that of Y^{3+}. It can also be found that the FWHM of the peaks in XRD patterns does not vary with the increase in Bi^{3+} content, namely, Bi^{3+} doping does not influence the crystallinity of Y_2O_3 which could affect the emission of Er^{3+}.

Fig. 2 shows the emission spectra of 1.0 mol% Er^{3+}:Y_2O_3 (Er^{3+}:Y_2O_3), 1.0 mol% Bi^{3+}:Y_2O_3 (Bi^{3+}:Y_2O_3) and 1.0 mol% Bi^{3+} codoped Er^{3+}:Y_2O_3. The strong emission band of Bi^{3+} locates at wavelengths from 360 to 630 nm, while the emission peaks of Er^{3+}:Y_2O_3 are very weak. However, the 1.0 mol% Bi^{3+} activated Er^{3+}:Y_2O_3 exhibits sharp peaks due to $^2H_{11/2}/^4S_{3/2} \rightarrow {}^4I_{15/2}$ transitions of Er^{3+} ions and its emission intensity is about 42 times larger than that of the sample without Bi^{3+}.

There are two main mechanisms for energy transfer between sensitizer and activator: (1) radiative transfer through emission of sensitizer and reabsorption by activator; (2) non-radiative transfer associated with resonance between absorber and emitter [13]. As shown in Fig. 3, the strong excitation band from 300 to 360 nm is attributed to the $^1S_0 \rightarrow {}^3P_1$ transition of Bi^{3+} while the excitation peaks at wavelength longer than 360 nm are ascribed to the $^4I_{15/2} \rightarrow {}^4F_{7/2}$ and $^4I_{15/2} \rightarrow {}^2H_{11/2}$ transitions of Er^{3+} [15,16]. The emission band of Bi^{3+} ranging from 360 to 630 nm significantly overlaps with the excitation spectrum of Er^{3+} ranging from 360 to 540 nm. Therefore, it can be concluded that in this system Bi^{3+} is a sensitizer for the luminescence of Er^{3+} and Bi^{3+} can transfer energy to Er^{3+} through the radiative transfer process. The luminescent intensity of Er^{3+} is remarkably enhanced by the incorporation of Bi^{3+} under 330 nm light excitation, which suggested a very efficient energy transfer from Bi^{3+} to Er^{3+}.

Fig. 4 shows the emission spectra of Er^{3+}:Y_2O_3 codoped with different amounts of Bi^{3+} (excited at 330 nm). In Fig. 4, the sharp emission peaks correspond to the $^2H_{11/2}/^4S_{3/2} \rightarrow {}^4I_{15/2}$ transitions of Er^{3+}. The position of emission peaks dose not vary with the Bi^{3+} concentration, but the luminescence intensity changes a lot. The inset displays the enhancement magnitude of the emission intensity of Er^{3+}, ranging from 515 to 580 nm, as a function of Bi^{3+} concentration. As shown in the inset, the intensity of Er^{3+} considerably increases first, reaches a maximum at the 2.0 mol% Bi^{3+}, and falls thereafter. The decrease in the emission intensity is caused by the concentration quenching of Bi^{3+}. The total energy transfer efficiency depends not only on the probability of energy transfer from sensitizer to activator, but also on that between the sensitizers [15,17]. The energy transfer efficiency increases with the decrease of the distance between the sensitizer and activator (or sensitizer). In this study, Bi^{3+} is the sensitizer and Er^{3+} is the activator. In the case of the Bi^{3+} content less than 2 mol%, the distance between Bi^{3+} and Er^{3+} decreases with Bi^{3+} doping, and thus the energy transfer efficiency from Bi^{3+} to Er^{3+} increases. However, when the concentration of Bi^{3+} exceeds 2.0 mol%, the average distance between two Bi^{3+} becomes short. This leads to the efficient energy transfer

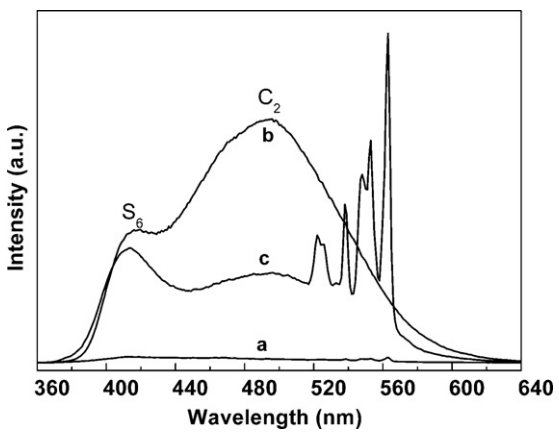

Fig. 2. Emission spectra of Er^{3+}:Y_2O_3 (a, excited at 330 nm), Bi^{3+}:Y_2O_3 (b, excited at 330 nm) and 1.0 mol% Bi^{3+} codoped Er^{3+}:Y_2O_3 (c, excited at 330 nm).

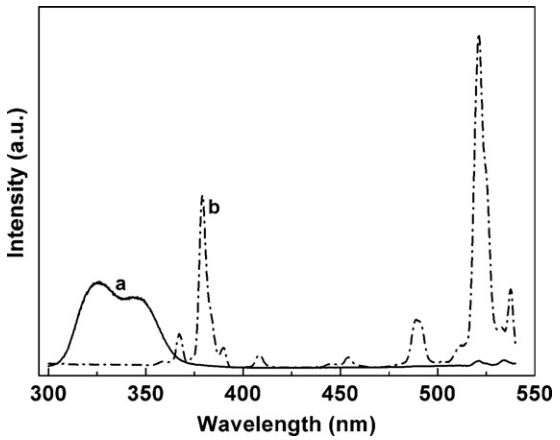

Fig. 3. Excitation spectra of Bi^{3+}:Y_2O_3 (a, monitored at 563 nm), Er^{3+}:Y_2O_3 (b, monitored at 563 nm).

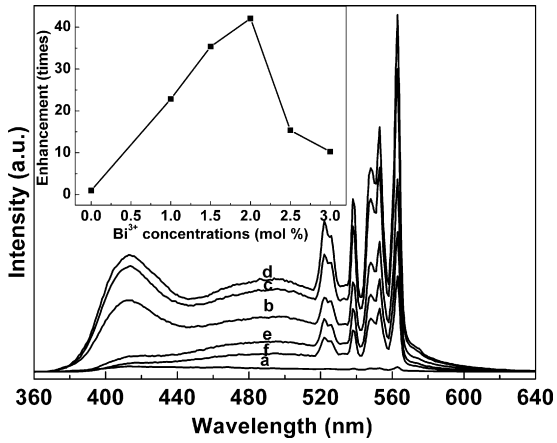

Fig. 4. Emission spectra of the Bi^{3+} and Er^{3+} codoped Y_2O_3 phosphors (with a fixed Er^{3+} concentration of 1.0 mol%, excited at 330 nm): (a) 0 mol% Bi^{3+}; (b) 1.0 mol% Bi^{3+}; (c) 1.5 mol% Bi^{3+}; (d) 2.0 mol% Bi^{3+}; (e) 2.5 mol% Bi^{3+}; (f) 3.0 mol% Bi^{3+}, the inset is the emission intensity of Er^3 as a function of the Bi^{3+} concentration.

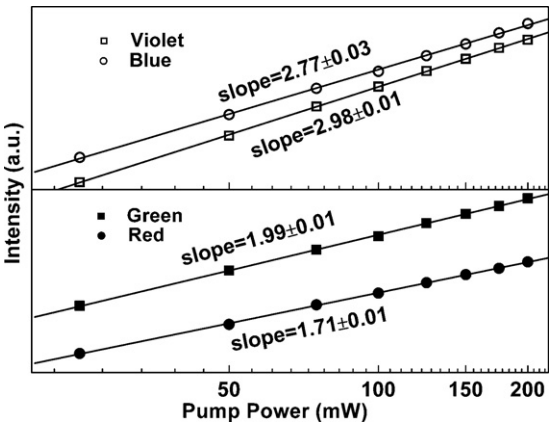

Fig. 6. The pump power dependence of the violet, blue, green and red upconversion emission intensity of 1.5 mol% Bi^{3+} codoped Er^{3+}:Y_2O_3.

between Bi^{3+}, and the non-radiative process increases gradually, which hinders the energy transfer from Bi^{3+} to Er^{3+}. In a word, adding an optimal amount of Bi^{3+} to Er^{3+}:Y_2O_3 can enhance the emission intensity of Er^{3+} through energy transfer from Bi^{3+} to Er^{3+}, but after exceeding the optimum concentration, the energy transfer between Bi^{3+} becomes more efficient which thus results in less energy transfer from Bi^{3+} to Er^{3+}.

As discussed above, an appropriate amount of Bi^{3+} doping can enhance emission intensity of Er^{3+}:Y_2O_3 through the radiative transfer process under UV excitation. In addition to UV excitation, the emission intensity of Er^{3+}:Y_2O_3 under IR excitation can also be increased by Bi^{3+} doping. Fig. 5a displays the upconversion luminescence spectra of the Er^{3+}/Bi^{3+} codoped Y_2O_3 under 980 nm excitation. The inset shows the integral intensity of green and red emissions as a function of Bi^{3+} content. As shown in the inset, both the green and red emissions increase as the Bi^{3+} content is below 1.5 mol%, however, above that concentration the emission intensity becomes weak. In order to clarify the mechanism of the change in green and red emissions depending on Bi^{3+} content, we measure the violet and blue emissions of Er^{3+}/Bi^{3+} codoped Y_2O_3 under excitation at 980 nm as well as the power dependence of violet, blue, green and red emissions. It is known that this dependence is expressed as $I \propto nP$, where I is the intensity of emission, P is the laser pump power, and n is the number of phonons needed to produce the emission [18].

Fig. 5b shows the violet and blue spectra of Er^{3+}/Bi^{3+} codoped Y_2O_3 under excitation at 980 nm. We cannot observe the emission band of Bi^{3+} in the upconversion spectra ranging from 350 to 480 nm. Moreover, as shown in Fig. 6, the values of slopes for the violet, blue, green and red emissions are 2.98, 2.77, 1.99 and 1.71, respectively. It indicates that both the violet and blue emissions are 3 phonon processes, and both the green and red emissions are 2 phonon processes. Consequently, the upconversion processes of Er^{3+}/Bi^{3+} codoped Y_2O_3 could be described as Fig. 7. The Er^{3+} can be promoted to the $^4I_{11/2}$ state through ground state absorption (GSA) process, and then nonradiative relaxation occurs and populates the $^4I_{13/2}$ state. Subsequently, $^4I_{11/2}$ and $^4I_{13/2}$ state are further excited to the $^4F_{7/2}$ and $^4F_{9/2}$ state respectively via excited state

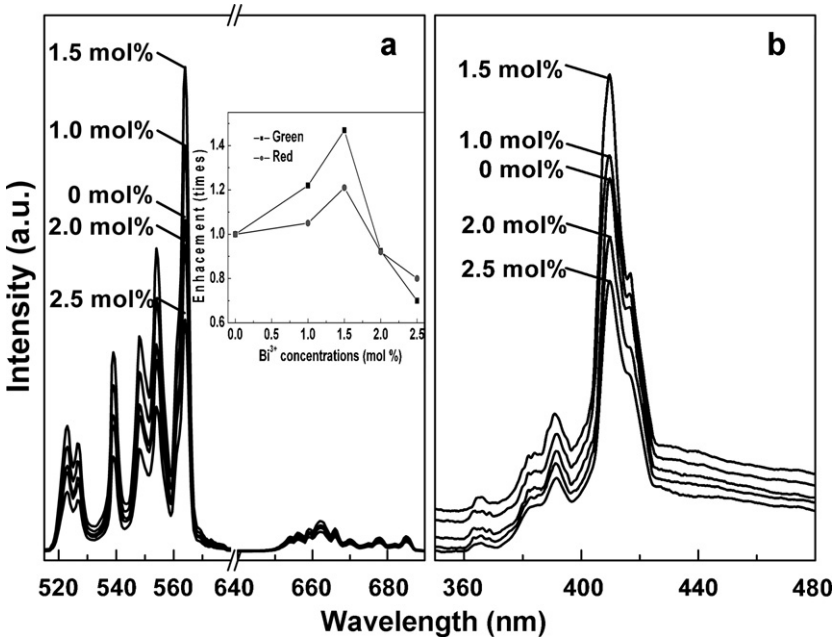

Fig. 5. Upconversion emissions of Er^{3+}:Y_2O_3 powders with different concentrations of Bi^{3+} under 980 nm excitation. The inset is the emission intensity as a function of the Bi^{3+} concentration.

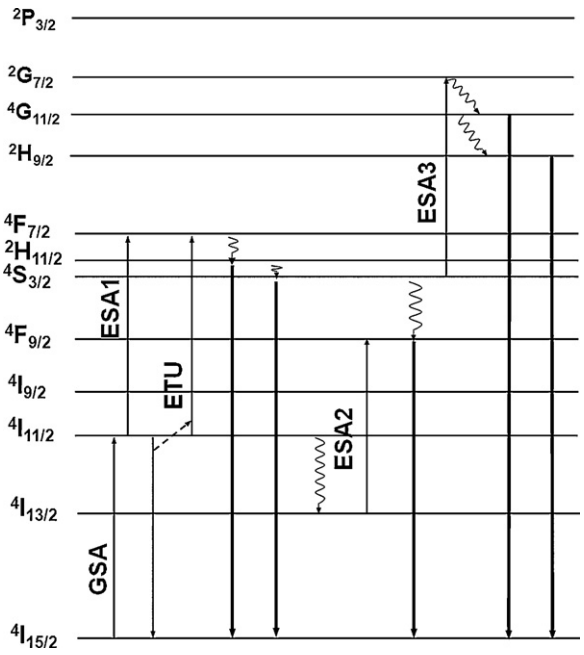

Fig. 7. Energy level diagram of Er^{3+} ion as well as the upconversion processes of the violet, blue, green and red emissions in 1.5 mol% Bi^{3+} codoped Er^{3+}:Y_2O_3 under 980 nm excitation.

absorption (ESA1 and ESA2) or energy transfer upconversion (ETU) processes. After that nonradiative relaxation processes populate the $^2H_{11/2}$/$^4S_{3/2}$ and $^4F_{9/2}$ states, so the green and red emissions are observed by the transitions of $^2H_{11/2}$/$^4S_{3/2}$→$^4I_{15/2}$ and $^4F_{9/2}$→$^4I_{15/2}$. The Er^{3+} ions in the $^4S_{3/2}$ state are excited to $^2G_{7/2}$ state by absorbing a third phonon (ESA3), and then nonradiatively relax to $^4G_{11/2}$, $^2H_{9/2}$ states. From these two states violet and blue emissions are emitted. As mentioned above, the doping of Bi^{3+} does not change the emission process of Er^{3+}, that is to say, there is not energy transfer between Bi^{3+} and Er^{3+} under 980 nm excitation. Moreover, high crystallinity could lessen nonradiative relaxation probability and then enhance the emission intensity of Er^{3+}. Nevertheless, from the XRD patterns we can conclude that Bi^{3+} doping does not influence the crystallinity of Er^{3+}/Bi^{3+} codoped Y_2O_3. Therefore, the enhanced emission of Er^{3+}/Bi^{3+} codoped Y_2O_3 originates from neither the energy transfer nor the crystallinity. It is well known that the intra-4*f* electronic transitions of rare earth are parity forbidden according to the quantum mechanical selection rules. However, the forbiddance can be partially broken when the rare earth situates at low symmetry sites [10,19]. The radius of Bi^{3+} (1.03 Å) is larger than that of Y^{3+} (0.90 Å) [20], so the substitution of Bi^{3+} for Y^{3+} can modify the symmetry of the crystal field in the lattice and enhance the radiative transition rate favoring the enhancement of upconversion emission intensity. The sensitization of upconversion emission of Er^{3+} on Bi^{3+} doping suggests that the Bi^{3+} could effectively modify the crystal field around Er^{3+} and the modification of crystal field depends strongly on the Bi^{3+} doping content. The optimal doping content of Bi^{3+} is found to be 1.5 mol%, and the corresponding emission intensity is 1.5 times larger than that without Bi^{3+} doping. When the Bi^{3+} content exceeds 1.5 mol%, the upconversion emission becomes weak due to the concentration quenching. For higher content of Bi^{3+}, Bi_n^{3+} aggregates may be formed [21], which act as trapping centers and dissipate the absorbed energy nonradiatively instead of transferring it to the Er^{3+} activator.

4. Conclusions

The enhancement of the emission in Er^{3+}/Bi^{3+} codoped Y_2O_3 under 330 nm and 980 nm results from two different mechanisms. The remarkably enhanced luminescent intensity under UV excitation originates from the efficient energy transfer from Bi^{3+} to Er^{3+}, whereas the enhancement in the upconversion emissions under IR excitation is attributed to the modification of the local crystal field around the Er^{3+}. The significant enhancement of emission intensity under both UV and IR excitations suggests that Er^{3+}/Bi^{3+}:Y_2O_3 could be a promising candidate in the application of optoelectronic devices.

Acknowledgments

This work was supported by the National Natural Science Foundation of China (Grant Nos. 50672019 and 10804024) and the Scientific Research Foundation for the Returned Overseas Chinese Scholars, State Education Ministry. Supported by "the Fundamental Research Funds for the Central Universities" (Grant No. HIT.NSRIF.2009056).

References

[1] X.D. Qi, C.M. Liu, C.C. Kuo, J. Alloys Compd. 492 (2010) L61.
[2] B.J. Chen, E.Y.B. Pun, H. Lin, J. Alloys Compd. 479 (2009) 352.
[3] S.F. Lim, R. Riehn, W.S. Ryu, N. Khanarian, C.K. Tung, D. Tank, R.H. Austin, Nano Lett. 6 (2006) 169.
[4] Q. Dong, G.J. Zhao, D.H. Cao, J.Y. Chen, Y.C. Ding, J. Alloys Compd. 493 (2010) 661.
[5] F. Vetrone, J.C. Boyer, J.A. Capobianco, A. Speghini, M. Bettinelli, Chem. Mater. 15 (2003) 2737.
[6] R. Srinivasan, N.R. Yogamalar, J. Elanchezhiyan, R.J. Joseyphus, A.C. Bose, J. Alloys Compd. 496 (2010) 472.
[7] Y.P. Li, J.H. Zhang, X. Zhang, Y.S. Luo, S.Z. Lu, Z.D. Hao, X.J. Wang, J. Phys. Chem. C 113 (2009) 17705.
[8] H.X. Zhou, Q.H. Yang, J. Xu, H.J. Zhang, J. Alloys Compd. 471 (2009) 474.
[9] Y.F. Bai, Y.X. Wang, G.Y. Peng, K. Yang, X.R. Zhang, Y.L. Song, J. Alloys Compd. 478 (2009) 676.
[10] M.Z. Yang, Y. Sui, S.P. Wang, X.J. Wang, Y.Q. Sheng, Z.G. Zhang, T.Q. Lü, W.F. Liu, Chem. Phys. Lett. 492 (2010) 40.
[11] T.S. Chan, C.C. Kang, R.S. Liu, L. Chen, X.N. Liu, J.J. Ding, J. Bao, C. Gao, J. Comb. Chem. 9 (2007) 343.
[12] S. Neeraj, N. Kijima, A.K. Cheetham, Solid State Commun. 131 (2004) 65.
[13] M.Q. Wang, X.P. Fan, G.H. Xiong, J. Phys. Chem. Solids 56 (1995) 859.
[14] L.G. Jacobsohn, M.W. Blair, S.C. Tornga, L.O. Brown, B.L. Bennett, R.E. Muenchausen, J. Appl. Phys. 104 (2008) 124303.
[15] Q.H. Xu, B.C. Lin, Y.L. Mao, J. Lumin. 128 (2008) 1965.
[16] L. Chen, H.W. Zheng, J.G. Cheng, P. Song, G.T. Yang, G.B. Zhang, C. Wu, J. Lumin. 128 (2008) 2027.
[17] K. Fujioka, T. Saiki, S. Motokoshi, Y. Fujimoto, H. Fujita, M. Nakatsuka, J. Lumin. 130 (2010) 455.
[18] G.Y. Chen, Y. Liu, Y.G. Zhang, G. Somesfalean, Z.G. Zhang, Q. Sun, F.P. Wang, Appl. Phys. Lett. 91 (2007) 133103.
[19] S.H. Shin, J.H. Kang, D.Y. Jeon, D.S. Zang, J. Lumin. 114 (2005) 275.
[20] R.D. Shannon, Acta. Cryst. A32 (1976) 751.
[21] X.L. Pang, Y. Zhang, L.H. Ding, Z.H. Su, W.F. Zhang, J. Nanosci. Nanotechnol. 10 (2010) 1860.